CrystEngComm

Discovery of new polymorphs of the tuberculosis drug isoniazid

Journal:	*CrystEngComm*
Manuscript ID	CE-COM-03-2020-000440
Article Type:	Communication
Date Submitted by the Author:	22-Mar-2020
Complete List of Authors:	Zhang, Keke; Tianjin University,, School of Chemical Engineering and Technology Fellah, Noalle; New York University, Shtukenberg, Alexander; New York University, Department of Chemistry Fu, Xiaoyan; Dalian Institute of Chemical Physics, Chinese Academy of Sciences Hu, Chunhua; New York University, Department of Chemistry Ward, Michael; New York University, Chemistry

COMMUNICATION

Discovery of new polymorphs of the tuberculosis drug isoniazid

Keke Zhang,[‡a,b] Noalle Fellah,[‡a,b] Alexander G. Shtukenberg,[a] Xiaoyan Fu,[c] Chunhua Hu,[a] Michael D. Ward*[a]

Received 00th January 20xx,
Accepted 00th January 20xx

DOI: 10.1039/x0xx00000x

Two new metastable polymorphs of the tuberculosis drug isoniazid, considered monomorphic for sixty years, were discovered using melt crystallization and nanoscale confinement. The two new forms are readily distinguished from the known form by optical microscopy, Raman spectroscopy and X-ray powder diffraction. A single crystal structure was obtained for one of the new polymorphs.

Tuberculosis (TB) has plagued mankind since prehistoric time,[1] today affecting more than 10 million and causing the death of 1.3 million people each year.[2] Shortly after the failure of the chemotherapeutic agent sodium glucosulfate to counter TB in the 1940s, the antibiotic streptomycin was found to be effective.[3,4] Streptomycin was accompanied by side effects as well as resistance development when administered alone, however, leading to the development of the antibiotics isoniazid, ethambutol, rifampicin and pyrazinamide during the next thirty years for TB treatment.[5] The development of resistance to TB drugs is a persistent problem, however,[2] and the World Health Organization (WHO) and International Union Against Tuberculosis Lung Disease (IUATLD) recommend the use of fixed-dose combinations (FDCs) wherein two or more active pharmaceutical ingredients are contained in a single dose.[6] These efforts dovetail with escalating development of known TB drugs as well as the search for new ones.

Isoniazid (INZ, also known as 4-Pyridinecarboxylic acid hydrazide, and isonicotinic acid hydrazide, Scheme 1) is a frontline antitubercular drug that is included among the World Health Organization List of Essential Medicines.[2] Introduced in 1952, it is typically combined with rifampicin, pyrazinamide and ethambutol in a FDC formulation.[7] The instability of INZ in tablets compromises efficacy, however, and the degradation is accelerated in the FDC tablets because of drug-drug interactions.[8-10] Recent studies have aimed to modulate INZ physicochemical properties, including morphology, solubility and bioavailability, through cocrystal forms of INZ or its crystallization in liposomes.[11-21] Efforts also have focused on the discovery of new polymorphs in an effort to improve chemical and physical properties. In the case of rifampicin and pyrazinamide, two polymorphs and four polymorphs are known, respectively.[22-25] INZ has been studied for more than half a century, yet only one polymorph has been reported to date.[26-29] A very recent investigation of isoniazid crystallization using tailored gelators and microemulsions concluded that isoniazid was “genuinely” monomorphic.[30] Herein we report the discovery and characterization of two new INZ polymorphs by crystallization from the melt and nanoconfinement, both simple yet powerful methods that our laboratory has used to discover new polymorphs of many common compounds.[31-36] The two new forms and the previously known form are readily distinguished by their remarkable morphologies and phase behavior, the understanding of which is essential for the development and certification of drugs like isoniazid, their bioavailability, and long-term shelf stability.

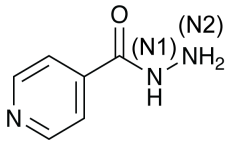

Scheme 1 Isoniazid (INZ)

[a] *Department of Chemistry and Molecular Design Institute, New York University, New York City, NY, 10003, USA. Email: mdw3@nyu.edu*
[b] *School of Chemical Engineering and Technology, State Key Laboratory of Chemical Engineering, Tianjin University, Tianjin 300072, People’s Republic of China.*
[c] *State Key Laboratory of Catalysis, Dalian Institute of Chemical Physics, Chinese Academy of Sciences, Dalian 116023, People’s Republic of China.*
‡ These authors contributed equally to this work.
Electronic Supplementary Information (ESI) available: Experimental and characterization details and additional figures. CCDC 1984160. For ESI and crystallographic data in CIF see DOI: 10.1039/x0xx00000x

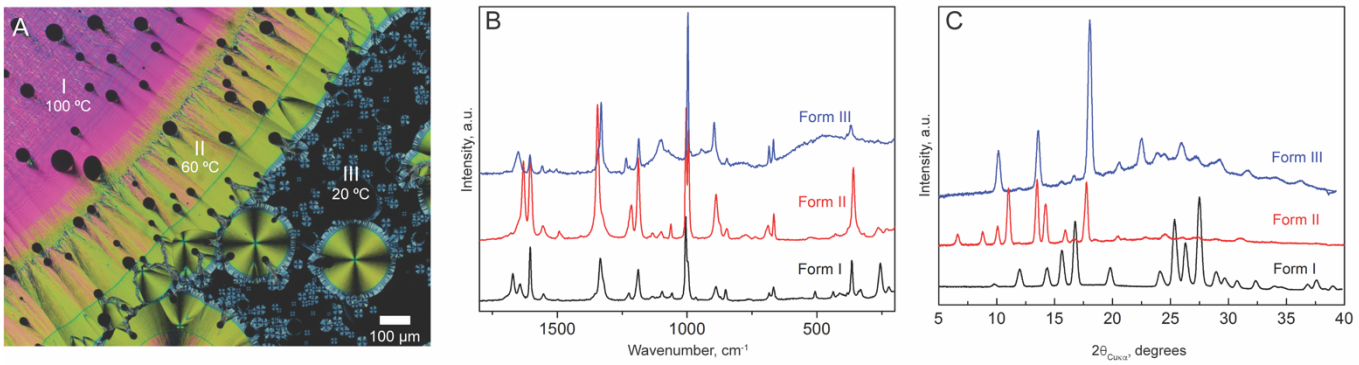

Fig. 1 (A) Polarized light micrograph of INZ crystallized from a melt confined between a microscope slide and glass coverslip. The confined INZ was melted on a Kofler bench at 180 °C, then cooled to 100 °C, resulting in the nucleation of Form **I**. The sample then was moved to the 60 °C zone on the Kofler bench, resulting in the formation of Form **II**. Form **III** was nucleated by moving the sample to a metal heat sink at ambient temperature. (B) Raman spectra of the INZ polymorphs. (C) Powder X-ray diffraction patterns of the INZ polymorphs.

Melt crystallization of INZ was performed by confining approximately 5 mg of INZ powder between a glass microscope slide and a glass coverslip, heating to 180 °C on a Kofler bench (the melting point of commercially obtained INZ was 170 °C), then cooling to different temperatures using the Kofler bench or quenching to room temperature by placing the sample onto an aluminum block that acted as a heat sink. This produced three crystalline polymorphs that were readily distinguishable under a polarized light microscope (Figure 1A). One form was identified by Raman spectroscopy and powder X-ray diffraction (Figures 1B, 1C and S1) as the known Form **I**, whereas the other two corresponded to two new polymorphs, denoted here as Form **II** (long flakes) and Form **III** (small spherulites). The Raman spectra and PXRD data indicate that the three forms are unequivocally distinct. The nucleation of each polymorph was strongly temperature dependent. Form **I** nucleated above 80 °C, Form **II** below 80 °C but above 30 °C, and Form **III** below 30 °C (Figure 1A). When confined between two glass slides at room temperature, Form **II** converted to Form **I** within several days. If the coverslip was removed at room temperature, Form **II** transformed to Form **I** within hours. Form **III** transformed to Form **I** at room temperature within several minutes when confined between the glass slide and coverslip, but in less than a minute when the coverslip was removed. These observations support a room temperature stability ranking **I > II > III**.

Sublimation of commercial INZ by heating under ambient pressure at 90°C for 24 hours produced needle-like crystals of Form **II** suitable for single crystal X-ray diffraction, accompanied by flaky crystals of Form **I** (Figure S2). The crystal structure of Form **II** was solved in the orthorhombic space group $Pca2_1$ with a = 34.428(5) Å, b = 3.8120(6) Å, c = 19.787(3) Å, V = 2596.8(7) Å^3, and Z = 16 (Table S1). The calculated powder X-ray diffraction pattern corresponds with the experimental pattern of Form **II** grown from the melt (Figure S5), confirming agreement between the single crystal structure and the thin film of Form **II**. The melting temperature of Form **II** determined by hot stage microscopy was 123–124 °C which is significantly lower than the melting point of Form **I** (170 °C). Attempts to obtain suitable single crystals of Form **III** for structure determination using a conventional X-ray diffractometer were unsuccessful due to the fast transformation of Form **III** to Form **I**. Higher resolution synchrotron powder diffraction data (Figure S6), however, enabled determination of the unit cell dimensions (9.754(5) Å, 8.568(4) Å, 3.931(2) Å, Z = 2), although the data was consistent with either an orthorhombic or monoclinic cell (see ESI).

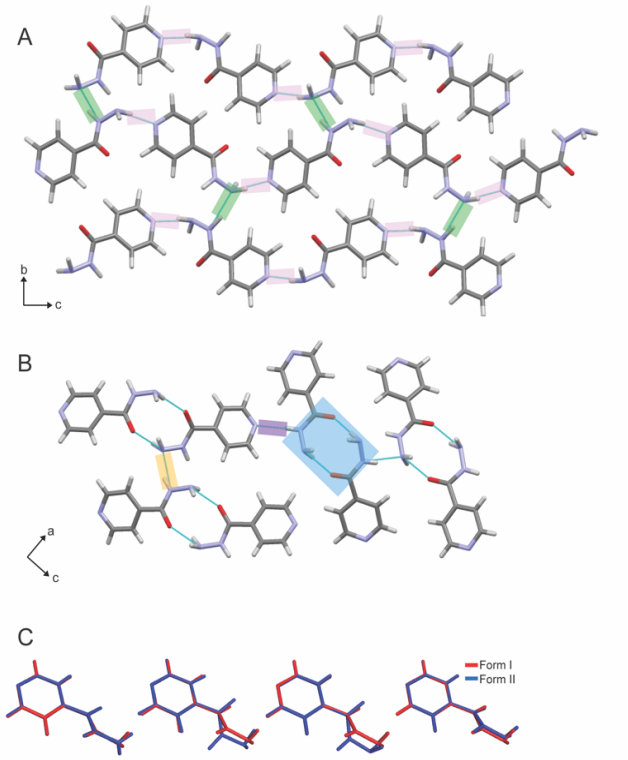

Fig. 2 Molecular arrangements of INZ molecules. (A) Form **I** viewed along the *a*-axis. Head-to-tail N2-H···N(pyridine) hydrogen bonds result in ribbons (pink). N2-H···N1 interactions (green area) between hydrazide groups connect the ribbons. (B) Form **II** viewed along the *b*-axis. Hydrogen-bonded N2-H···O dimers (blue) are linked by head-to-tail N1-H···N(pyridine) interactions (purple) and N2-H···N1 interactions between hydrazide groups (yellow). (C) Overlay of INZ molecule in Z' = 1 Form **I** (red) on the four independent molecules of Z' = 4 Form **II** (blue) from experimental single crystal structure. N1 and N2 denote the hydrazide nitrogen atoms in Scheme 1.

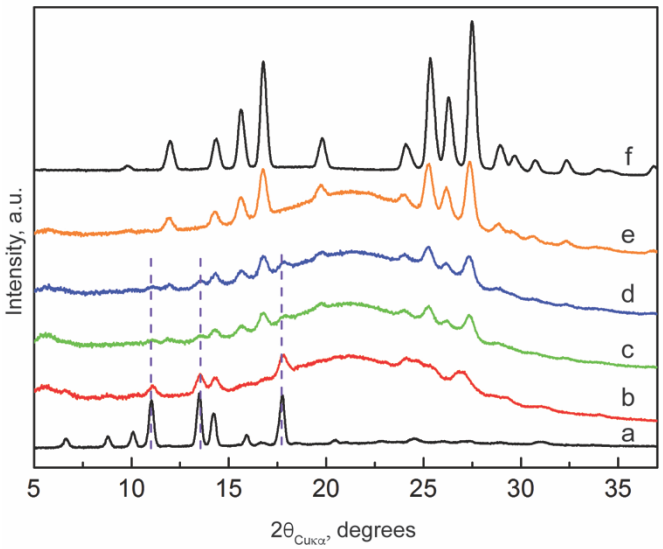

Fig. 3 X-ray diffraction patterns of INZ nanocrystals embedded in (b) 30 nm, (c) 50 nm, (d) 100 nm and (e) 140 nm CPG. (a) and (f) are INZ bulk Forms **II** and **I**, respectively.

The hydrogen bond motifs of INZ Forms **I** and **II** differ. Both polymorphs exhibit infinite hydrogen bonded chains, but only Form **II** exhibits hydrogen bonded dimers. INZ molecules in Form **I** form head-to-tail N2-H···N(pyridine) hydrogen bonds (pink area in Figure 2A) in undulating ribbons along the *c* direction. The ribbons are connected to each other by N2-H···N1 interactions (green area in Figure 2A) between hydrazide groups. Form **II** is described by two crystallographically independent dimers formed from N2-H···O hydrogen bonds (blue area in Figure 2B). These dimers are linked together by head-to-tail N1-H···N(pyridine) interactions (purple area in Figure 2B) and N2-H···N1 interactions (yellow area in Figure 2B) between hydrazide groups. The asymmetric unit of Form **II** contains four molecules (*Z'* = 4), compared to one in Form **I** (*Z'* = 1). The torsion angles of the independent molecules in Form **II** differ from those in Form **I** as well (Figure 2C, Table S2).

The lattice energies of INZ Form **I** (ref code INICAC03) and Form **II** were calculated using Vienna Ab Initio Simulation Package (VASP 5.3.5),[37] using density functional theory (DFT). The energy cutoff was 500eV for the expansion of plane wave, which was described using the projector-augmented wave (PAW) method.[38] The generalized gradient approximation (GGA)[39] of a revised Perdew–Burke–Ernzerhof (rPBE) functional[40] was employed to account for electronic exchange and correlation. The D2 method of Grimme was used to estimate van der Waals forces.[41] Monkhorst–Pack mesh of (5 × 2 × 1), (1 × 1 × 1) and (2 × 2 × 1) k-points was used for Brillouin zone integration and geometry optimizations, and the convergence criterion was set at 0.01 eV/Å. The calculations predict lower lattice energy for Form **I** compared with Form **II** (-26.456 *vs*. -25.415 kcal/mol, respectively), which agrees with the greater stability of Form **I** observed experimentally. The calculated values of the torsion angles, τ_1 and τ_2 in the DFT optimized structures agree well with the experimental values (Figure 2C, Table S2).

Our laboratory has demonstrated that crystallization under nanoconfinement is an effective method for the discovery of new polymorphs and stabilization of metastable forms.[42,43] INZ crystallization from the melt in controlled pore glass (CPG) with pore sizes ranging from 4 to 200 nm pore sizes afforded Form **I** in 140-200 nm, as determined by powder X-ray diffraction of the confined crystals (Figure 3). In contrast, Form **II** crystallized in 30-100 nm pores, although it transformed to Form **I** within hours. Below 8 nm, INZ existed in an amorphous state for at least two months, eventually transforming to Form **I**.

In conclusion, crystal morphology, growth characteristics, PXRD, Raman spectroscopy and single crystal X-ray diffraction unequivocally prove the existence of two new polymorphs of INZ obtained by crystallization from the melt, a surprising discovery given that INZ has been considered monomorphic (as now Form **I**) for more than 60 years. The single crystal structure of Form **II** is characterized by hydrogen bond motifs that differ from the more stable Form **I**. The results illustrate that melt crystallization and crystallization under nanoconfinement are promising experimental methods for polymorph screening, which is critical for the development and efficacy of active pharmaceutical ingredients. This is particularly important for high *Z'* structures that may not be tested by computational crystal structure prediction methods. Moreover, these results further support the conjecture by McCrone that "in general, the number of forms known for a given compound is proportional to the time and money spent in research on that compound."[44]

Acknowledgements. This work was supported by the National Science Foundation through award number DMR-1708716 and the New York University Materials Research Science and Engineering Center (MRSEC) program of the National Science Foundation under award number DMR-1420073. The authors are grateful for support from the U.S. National Science Foundation, award number DMR 1708716. The X-ray microdiffractometer with GADDS was acquired through the support of the National Science Foundation under Award Number CRIF/CHE-0840277 and NSF MRSEC Program under Award Number DMR-0820341. 35 Use of the Advanced Photon Source (APS) at Argonne National Laboratory was supported by the U. S. Department of Energy, Office of Science, Office of Basic Energy Sciences, under Contract No. DE-AC02-06CH11357. The authors are grateful to Dr. Wenqian Xu for providing assistance in collecting synchrotron powder diffraction data at APS. K. Zhang thanks the financial support from the China Scholarship Council.

Conflicts of interest

There are no conflicts to declare.

Notes and references

1 I. Hershkovitz, H. D. Donoghue, D. E. Minnikin, H. May, O. Y. C. Lee, M. Feldman, E. Galili, M. Spigelman, B. M. Rothschild and G. K. Bar-Gal, *Tuberculosis*, 2015, **95**, S122-S126.

2 World Health Organization. (2018). Global tuberculosis report 2018. World Health Organization.
3 J.H. Comroe Jr., *Am. Rev. Respir. Dis* 1978, **117**, 773-781.
4 W. H. Feldman, H. C. Hinshaw and F. C. Mann, *Am. Rev. Tuberc.*, 1945, **52**, 269-298.
5 J. F. Murray, D. E. Schraufnagel, P. C. Hopewell, *Ann Am Thorac Soc.* 2015, **12**, 1749–1759.
6 B. Blomberg, S. Spinaci, B. Fourie, R. Laing, *Bull. World Health Organ.* 2001, **79**, 1, 61-8.
7 C. Vilchèze, W. R. Jacobs, Jr, *Annu. Rev. Microbiol.* 2007, **61**, 35-50.
8 H. Bhutani, T. T. Mariappan, Saranjit Singh, *Drug Dev. Ind. Pharm.* 2004, **30**, 6, 667-672.
9 H. Bhutani, Saranjit Singh, K. C. Jindal, *Pharm. Dev. Technol.* 2005, **10**, 4, 517-524.
10 S. Singh, B. Mohan, *Int. J. Tuberc. Lung Dis.* 2003, **7**, 3, 298-303.
11 A. Lemmerer, J. Bernstein, V. Kahlenberg, *CrystEngComm*. 2010, **12**, 2856–2864.
12 A. Lemmerer, J. Bernstein, V. Kahlenberg, *J Chem Crystallogr*. 2011, **41**, 991–997.
13 A. Lemmerer, J. Bernstein, V. Kahlenberg, *CrystEngComm*. 2011, **13**, 5692–5708.
14 S. Aitipamula, A. B. Wong, P. S. Chow and R. B. J. C. Tan, 2013, **15**, 5877-5887.
15 B. Swapna, D. Maddileti, A. Nangia, *Cryst. Growth Des.* 2014, **14**, 5991−6005.
16 B. Yadav, A. Gunnam, R. Thipparaboina, A. K. Nangia, N. R. Shastri, *Cryst. Growth Des.* 2019, **19**, 5161−5172.
17 D. Han, T. Karmakar, Z. Bjelobrk, J. Gong, M. Parrinello, *Chem. Eng. Sci.* 2018, **204**, 320-328.
18 T. Gong, D. Han, Y. Chen, S. Wang, W. Tang, *J. Chem. Eng. Data* 2018, **63**, 12, 4767-4778.
19 R. Heryanto, E. C. Abdullah, M. Hasan, *J. Chem. Eng. Data* 2010, **55**, 6, 2306-2309.
20 B. Xuan, S. N. Wong, Y. Zhang, J. Weng, H. H. Y. Tong, C. Wang, C. C. Sun and S. F. Chow, *Cryst. Growth Des.*, 2020, **20**, 1951-1960.
21 C. I. Nkanga, R. W. Krause, X. S. Noundou and R. B. Walker, *Int. J. Pharm.*, 2017, **526**, 466-473.
22 S. Q. Henwood, W. Liebenberg, L. R. Tiedt, A. P. Lötter and M. M. de Villiers, *Drug Dev. Ind. Pharm.* 2001, **27**, 1017-1030.
23 A. L. Ibiapino, R. C. Seiceira, A. Pitaluga, A. C. Trindade and F. F. Ferreira, *CrystEngComm.* 2014, **16**, 8555-8562.
24 L. de Pinho Pessoa Nogueira, Y. S. de Oliveira, J. de C. Fonseca, W. S. Costa, F. N. Raffin, J. Ellena and A. P. Ayala, *J. Mol. Struct.* 2018, **1155**, 260-266.
25 S. Cherukuvada, R. Thakuria, A. Nangia, *Cryst. Growth Des.* 2010, 10, 9, 3931–3941.
26 L. H. Jensen, *J. Am. Chem. Soc.* 1954, **76**, 4463-4467.
27 T. N. Bhat, T. P. Singh, M. Vijayan, *Acta Cryst.* 1974, B30, 2921.
28 A. Lemmerer, *CrystEngComm* 2012, **14**, 2465-2478.
29 G. Rajalakshmi, V. R. Hathwar, P. Kumaradhas, *Acta Cryst.* 2014, **B70**, 331–341.
30 S. R. Kennedy, C. D. Jones, D. S. Yufit, C. E. Nicholson, S. J. Cooper and J. W. Steed, *CrystEngComm.*, 2018, **20**, 1390-1398.
31 N. Fellah, A. G. Shtukenberg, E. J. Chan, L. Vogt-Maranto, W. Xu, C. Li, M. E. Tuckerman, B. Kahr and M. D. Ward, *Cryst. Growth Des.*, 2020, DOI: 10.1021/acs.cgd.0c00096.
32 A. G. Shtukenberg, Q, Zhu, D. J. Carter, L. Vogt, J. Hoja, E. Schneider, H. Song, B. Pokroy, I. Polishchuk, A. Tkatchenko, A. R. Oganov, A. L. Rohl, M. E. Tuckerman, B. Kahr, *Chem. Sci.* 2017, **8**, 4926-4940.
33 A. G. Shtukenberg, C. T. Hu, Q. Zhu, M. U. Schmidt, W. Xu, M. Tan, B. Kahr, *Cryst. Growth Des*., 2017, **17**, 3562−3566.
34 J. Yang, C. T. Hu, A. G. Shtukenberg, Q. Yin, B. Kahr, *CrystEngComm* 2018, **20**, 1383-1389.
35 A. G. Shtukenberg, M. Tan, L. Vogt-Maranto, E. J. Chan, W. Xu, J. Yang, M. E. Tuckerman, C. T. Hu, B. Kahr, *Cryst. Growth Des.* 2019, **19**, 4070-4080.
36 J. Yang, C. T. Hu, X. Zhu, Q. Zhu, M. D. Ward, B.Kahr, *Angew. Chem.* 2017, 10299-10303.
37 G. Kresse, J. Furthmüller, *Phys. Rev. B* 1996, **54**, 11169.
38 P. E. Blöchl, J. Kästner, C. J. Först, *Handbook of Materials Modeling* 2005, 93–119.
39 J. P. Perdew, J. A. Chevary, S. H. Vosko, K. A. Jackson, M. R. Pederson, D. J. Singh, C. Fiolhais, *Phys. Rev. B* 1993, **48**, 4978.
40 B. Hammer, J. K. Nørskov, *Phys. Rev. B* 1999, **59**, 7413.
41 S. Grimme, *J. Comp. Chem.* 2006, **27**, 1787.
42 J. M. Ha, B. D. Hamilton, M. A. Hillmyer, M. D. Ward, *Cryst. Growth Des.* 2009, **9**, 11, 4766-4777
43 B. D. Hamilton, M. A. Hillmyer, M. D. Ward, *Cryst. Growth Des.* 2008, **8**, 3368–3375.
44 W. C. McCrone, in *Physics and Chemistry of the Organic Solid State*, ed. D. Fox, M. M. Labes and A. Weissberger, Interscience Publishers, London, 1965, vol. 2, pp. 725-767.

